Prediction of size-dependent risk of salmon smolt (*Salmo salar*) escape through fish farm nets

Manu Sistiaga[a],[1], Bent Herrmann[a],[b],[*],[1], Eskil Forås[c], Kevin Frank[a], Leif Magne Sunde[a]

[a] *SINTEF Ocean, Brattørkaia 17C, N-7010 Trondheim, Norway*
[b] *The Arctic University of Norway, UiT, Breivika, N-9037 Tromsø, Norway*
[c] *AquaOptima AS, C/O Aqualine AS, Postbox 2200, N-7042 Trondheim, Norway*

ABSTRACT

The escape of small smolt through farm cage netting is a major challenge faced by the Norwegian salmon farming industry. Escape can occur when the smolt placed in the cages are smaller than the size estimated by the farmers. Furthermore, one may assume wrong mesh-properties as the cage netting change shape and/or state from stiff (mesh bars with tension) to slack (mesh bars without tension) due to sea currents or waves and become more suitable for penetration. The latter represents an increased risk for cages placed in more exposed sea areas, which is a growing trend in the industry due to increased demand for farming sites. The potential influence of mesh shape and state on the risk of escape from salmon farm cages is predicted. The morphological characteristics of salmon smolt are assessed and used to determine the risk of potential escape through meshes of different sizes, shapes and states. The results showed that fish smaller than 47 g and 201 g have the potential to escape through 30 mm and 50 mm meshes, respectively. In general, the risk of smolt escape is highest when the meshes in the netting are slack. Semi-slack meshes with mesh openness of between 65 and 95 % also present a higher risk of smolt escape than square stiff meshes. The highest risk of escape was identified at approximately 80 % mesh openness. This study illustrates the importance of mesh states in fish farming cage nettings. In many cases the minimum smolt size needed to maintain an escape risk below 1 % was approximately twice as large for slack square meshes than for stiff square meshes of the same size.

1. Introduction

Norway is known for its seafood products and has a well-developed Atlantic salmon (*Salmo salar*) farming industry. This industry has grown rapidly in the last 20 years, with total production increasing from 362,000 metric tons in 1998 to 1,237,000 metric tons in 2017 (Norwegian Directorate of Fisheries, 2018). In 2017, the export of salmon from Norway constituted 40 % of the total export volume of seafood, but this volume corresponded to 72 % of the total monetary value, which shows the importance and value of this industry to Norwegian society (Norwegian Seafood Council, 2018). Norwegian salmon farming is an industrial, economic, and to a certain extent, social success story. The industry has not only contributed to the economic growth of the country but has also facilitated the development of many coastal communities (Rybråten et al., 2018). However, the growth of the industry has also brought challenges. One of these challenges is finding suitable sites for the growing number of salmon farms in

Norway's fjords and coastal zones. This has led to the increased use of more exposed sea locations for salmon production. These exposed locations result in higher loads on the net cages due to strong water currents and large waves (Moe et al., 2010).

Norwegian Salmon farming is almost entirely carried out in net cages, and currently there are approximately 3600 salmon and trout *Oncorhynchus mykiss*) cages present in the Norwegian fjords (Norwegian Fisheries Directorate, 2018). The escape of fish from these cages is a serious issue for the fish farming industry in general, not only due to the economic loss for fish farmers but also because of the environmental threat it poses to wild salmon (Karlsson et al., 2016; Keyser et al., 2018). According to the Norwegian fisheries directorate (2018), approximately 300,000 salmon escaped per annum from Norwegian sea cages between 2001 and 2017. Apart from the economic cost of this loss, the fish that escape and survive add a societal cost in the form of environmental impact (e.g. genetic contamination of the rivers in the area).

* Corresponding author at: SINTEF Ocean, Brattørkaia 17C, N-7010 Trondheim, Norway.
E-mail address: Bent.Herrmann@sintef.no (B. Herrmann).
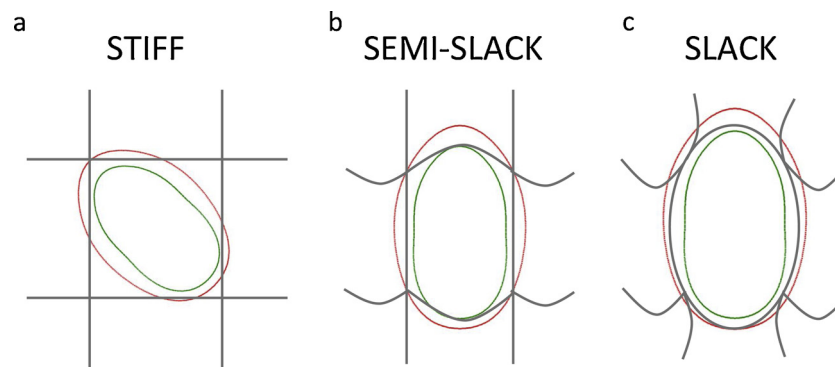[1] Equal authorship.

Fig. 1. Mesh penetration of a smolt represented by its cross section (red = uncompressed, green = maximum compression) through a stiff (a), semi-slack (b) and slack (c) mesh. (For interpretation of the references to colour in this figure legend, the reader is referred to the web version of this article).

Fish can escape from salmon cages for various reasons (Jensen et al., 2010). The most obvious and unpredictable is accidental opening that allows the salmon to swim out of the netting. The only way of decreasing the occurrence of fish escaping by this means is to improve work practices and equipment to reduce the risk of accidents (Bridger et al., 2015). Salmon can also escape through cage netting if the mesh is inappropriately sized according to smolt size. Therefore, finding the optimal mesh size for different scenarios (smolt minimum sizes vs. mesh properties) is critical for the industry. While mesh size in the cages is fully defined by the netting used, the mesh shape is less well defined because it is not only affected by how the netting is initially mounted on the cages, but also by the dynamics of the netting when exposed to varying sea conditions. Seawater currents and sea surface waves can dynamically distort the overall shape of the cage netting (Huang et al., 2006; Lader et al., 2003, 2008) and therefore, also the shape of the individual meshes and state of the mesh bars (taut or slack). These mesh state alterations in the netting may lead to changes in the minimum size of smolt required to prevent escape. Fisheries studies have shown that apart from mesh size, mesh shape and mesh bar state can affect which sizes of fish of a specific species can escape through a netting mesh (e.g. Herrmann et al., 2016a). Therefore, the same can be expected regarding potential escape of salmon smolt through meshes in fish farm cages.

In Norway, the fish farming industry and management authorities have carried out preliminary trials to establish smolt size limits to be used in cages with different mesh sizes (Harboe and Skulstad, 2013). However, the methods applied in these trials were limited and did not provide general guidelines that are applicable to different scenarios, regarding varying mesh shape and state. Further, these tests were carried out on free swimming fish, and do not represent conditions during processes such as delousing or net cleaning, where mesh shape can vary and fish can be forced through the netting (Moring, 1989). These crowding scenarios are similar to the retention/escape situations observed in trawls and seines, where the probability of fish penetrating the meshes in the codend increases with fish density and reduced distance to the netting panels (Reeves et al., 1992; Wienbeck et al., 2011).

The most commonly used nets in Norwegian salmon farming cages are made of square meshes of either 30 mm (15 mm bar length) or 50 mm (25 mm bar length) mesh size (2–3 mm polyamide twine) (Moe et al., 2007), depending on the sizes of fish that the cage is intended to hold. The present study aims to predict escape risk for salmon smolt through cage netting with different mesh sizes in different states. The study specifically aims to answer the following research questions:

1 What is the minimum size of smolt needed to avoid escape through 30 and 50 mm square mesh nets often employed by the salmon farming industry? And, how does mesh state affect the required minimum smolt size?
2 What is the minimum smolt size that can be safely deployed in a farm cage without risking escape through meshes of specific size and

state?

2. Materials and methods

2.1. Effect of mesh shape and state vs. smolt size and morphology on potential escape through cage netting

For smolt to pass through cage netting two conditions need to be fulfilled. Firstly, the smolt needs to "contact" the netting at an orientation that gives it a size-dependent possibility of passing through the mesh of the netting (Sistiaga et al., 2010). Secondly, the smolt needs to be morphologically able to pass through the mesh. Therefore, the main factors to consider in the escape risk of smolt from fish farming cages are mesh size, shape and state in relation to smolt size and morphology and tissue compressibility.

To investigate the size limits at which smolt cannot escape from certain net mesh sizes, the industry carries out penetration tests (Harboe and Skulstad, 2013). In these trials, individuals of a range of sizes are tested on the stretched (stiff) square meshes (Fig. 1a) of the cage to see if they are able pass through them. However, the meshes in the netting of a salmon cage are flexible, meaning that they can be deformed and adopt different shapes depending on the magnitude and direction of the forces they are exposed to. These forces depend on factors such as weather and sea currents (Huang et al., 2006; Lader et al., 2003, 2008), meaning that the mesh state in the netting of cages in exposed locations changes frequently, and the meshes often tend to be in semi-slack and slack states (Fig. 1). In addition, many of the operations carried out in farming cages involve the manipulation of the cage netting, which again results in the meshes in the netting adopting semi-slack or slack states. In a square mesh net panel hanging at sea, the load in the netting is on the vertical bars due to gravity, meaning that the horizontal bars are to a certain extent tensionless, and therefore deformable. This leads to a situation with semi-slack meshes where smolt could potentially deform the horizontal bars in the meshes in the process of squeezing itself through and finally escaping (Fig. 1b). At the same time, in situations where the sea state and water currents are strong enough to deform the netting, the load on the vertical bars would disappear, making the meshes slack and deformable in all directions (Fig. 1c). It is expected that slack, and at least some states of semi-slack, meshes would lead to a higher risk of escape for salmon smolt, simply because the mesh totally (slack) or partially (semi-slack) deforms when adjusting to the shape of smolt trying to squeeze through. Therefore, assuming a stable stiff state of the meshes in cage netting could lead to a serious underestimation of the minimum smolt size required to avoid the risk of escape.

Two factors determine the maximum size at which a smolt would be able to squeeze through a mesh. One is the deformability of the meshes in the netting and the other is the deformability or compressibility of the smolt tissue. This is illustrated in Fig. 1, where only a smolt with a
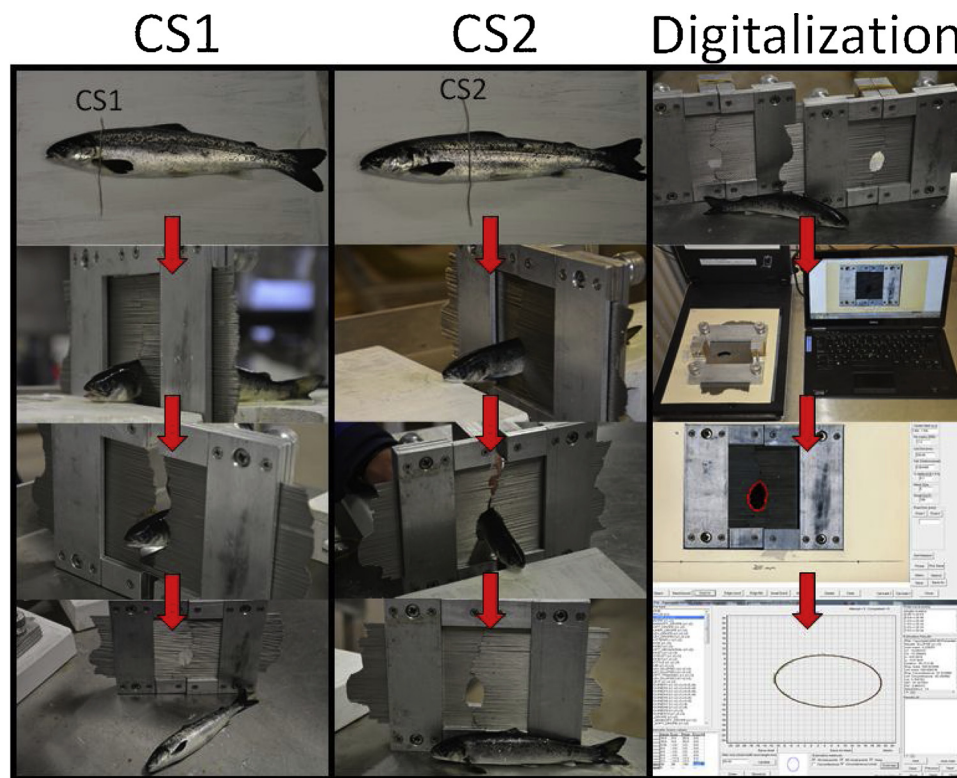
Fig. 2. The first and second column describe CS1 and CS2. The third column shows the process of digitization of the shapes measured by a morphometer.

compressibility level illustrated by the green cross section (CS) would be able to pass through the square meshes in each of the mesh states (Fig. 1a-c). Thus, to quantify the potential risk of escape for a smolt through a specific netting it is necessary to consider different potential netting scenarios in combination with the morphology and cross-sectional compressibility of the species being investigated.

2.2. FISHSELECT methodology and data collection

FISHSELECT (Herrmann et al., 2009, 2012) is a framework of methods, tools, and software developed to determine if a fish can penetrate a certain mesh or defined shape. The method has been widely used to study fishing gear size selectivity (the fish size-dependent probability for escape/retention) (Krag et al., 2011; Sistiaga et al., 2011). In the current study, this method was applied for the first time to predict the risk of smolt escaping through farm cage netting.

To study the size selectivity of a species using this method, both FISHSELECT software and specific measuring tools are needed (Fig. 2). Through computer simulation, the method estimates selectivity parameters comparing the morphological characteristics of a particular fish species and the shape and size of the selection devices of interest.

The following subsections briefly describe the different steps needed to use FISHSELECT. A more thorough description of the method can be found in Herrmann et al. (2009, 2012).

2.2.1. FISHSELECT morphometric data collection

In addition to measuring the length and weight of each individual smolt included in the study, the cross-sectional morphology of each smolt was measured. To obtain the correct morphometric measures for each fish using FISHSELECT, it is very important that the shape of the fish measured is not affected by dehydration, depressurization, rigor mortis, or any other factor that could alter the original shape of the fish. Therefore, the fish for the trials were handpicked in batches of 4 or 5 fish and killed with an overdose of MS 222 anaesthetic just before use. The aim with FISHSELECT is to make predictions for mesh penetration probability for the widest possible range of fish sizes. Thus, the method requires that the morphometric characteristics of the largest possible size range is measured. In the current study, apart from the condition of the smolt selected, the only other selection criteria for fish was that they covered the widest possible size range of fish.

Two cross sections were selected for their potential to determine fish passage through a mesh: cross section 1 (CS1), which is located directly behind the operculum, and cross section 2 (CS2), which is located at the point of the maximum transverse perimeter, the foremost point of the dorsal fin (Fig. 2). CS1 represents the point at which the bony structure in the head had its maximum girth, whereas CS2 was selected because it represents the point with maximum girth of the fish overall. Thus, these two CSs were expected to be the decisive CSs for mesh penetration.

The two cross-sections were measured using a sensing tool called a morphometer. The shapes formed in the morphometer were then scanned to obtain digital images of the contours using a flatbed scanner (Fig. 2).

Models, i.e. numerical representations through parametric shapes, of the digitized cross-sectional images obtained for each smolt were developed. For each CS, seven different shape models were considered: bottle, ellipse, flexellipse1, flexellipse2, flexelipse3, flexdrope2 and ship. AIC-value (Akaike, 1974) and R^2-values were calculated for each of the seven models for both CS1 and CS2 (see Tokaç et al., 2016 for further details on this process). The shape model with the lowest mean AIC-value was chosen to describe each of the two cross sections separately. The mean R^2-value was applied to judge how well the selected models on average described the cross-sectional shapes of salmon smolt. The relationship between total length and cross-section shape parameters was modelled for the most suitable shapes found for CS1 and CS2 separately. Based on these relationships, CS1 and CS2 for a virtual population of 5000 smolt with length uniformly distributed between 0 cm and 40 cm were simulated and subsequently used in the simulation of smolt size selection. This upper limit was selected because salmon above this size would certainly not be available during the experimental sampling.
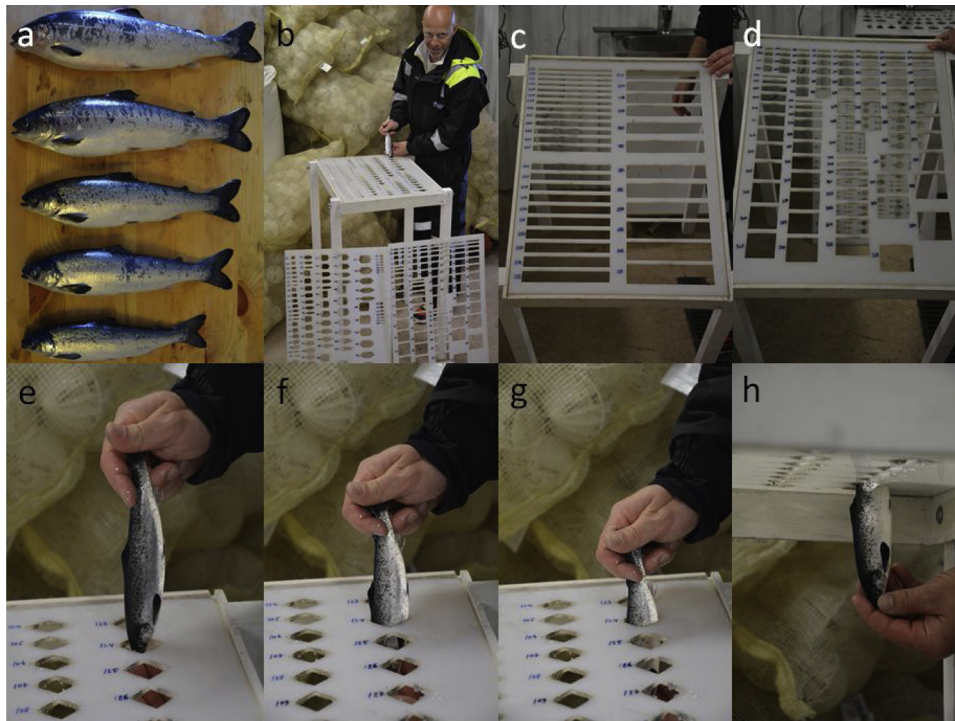
Fig. 3. Photo "a" shows the different smolt sizes used in the fall-through tests, photos "b-d" show the different templates employed in the fall-through tests, while photos "e-h" illustrate the fall-through procedure for a specific smolt and mesh.

2.2.2. Fall-through experiments

After measuring smolt morphology, fall-through experiments were carried out to determine whether each smolt included in the study could or could not physically pass through an array of stiff mesh shapes in 5 mm nylon-plate templates. Only the force of gravity was used to simulate the attempted penetration of smolt through the mesh (Fig. 3). The set of mesh templates used in this experiment comprised a total of 478 different shapes, representing mesh sizes from 20 to 245 mm. The shapes included diamonds (252 meshes), hexagons (98 meshes) and rectangles (128 meshes) and were identical to those described by Tokaç et al. (2016). All smolt were manually presented at an optimal orientation for mesh penetration to each of the 478 meshes in the templates. Penetration (Yes) or retention (No) was recorded for each smolt (see Hermann et al., (2009) for further details on the procedure). The purpose of the fall-through experiments was to be able to estimate the maximum compressibility for a smolt trying to squeeze itself through a mesh (see Herrmann et al. (2009) for further details).

2.2.3. Simulation of mesh penetration and selection of a penetration model

The shape and compressibility of a smolt determines whether or not a smolt will be able to pass through a mesh. The penetration models implemented in FISHSELECT simulate the compressibility of each smolt at each cross section. Visual and tactile inspection of the deformability of salmon smolt revealed that the dorsal and ventral compressibility of this species are different. For example, the ventral compressibility of smolt at CS2 was clearly much higher than the dorsal compressibility. Therefore, a model that allows asymmetrical compression for both CS1 and CS2 was applied. This model was previously used for redfish (*Sebastes* spp.) by Herrmann et al. (2012) and includes the estimation of three parameters, representing the dorsal, lateral and ventral compressibility of the fish. The potential compressibility of the fish at an arbitrary angle around the fish cross-section was then modelled by linear interpolation between the potential compressibility (dorsally, laterally and ventrally) of the fish at each cross-section (See Herrmann et al., 2009 for further details). In order to establish an optimal penetration model for salmon smolt, each CS1 and CS2 measurement, both

individually and in combination, was tested with different compression models using different values for the assumed dorsal, lateral and ventral compression. The penetration of the modelled CS1 and CS2 shapes of each smolt through the 478 different mesh templates used in the fall-through trials was simulated using the FISHSELECT software. The purpose of these simulations was to estimate the exact compression potential of the cross-sections and to assess which cross-section combinations needed to be considered when estimating the ability of salmon smolt to pass through meshes of different sizes and shapes. Models considering one cross-section at a time were created. For CS1, the dorsal, lateral and ventral compression varied from 0 to 30 %, 0–20% and 0–20%, respectively, in increments of 5 %. This resulted in a total of 245 penetration models for CS1. For CS2, the dorsal, lateral and ventral compression varied from 0 to 30 %, 0–20% and 0–40%, respectively, in increments of 5 %. This resulted in a total of 315 penetration models for CS2. In addition to the models run for each cross section, 77,175 models where CS1 and CS2 were combined were also tested. Each compression model was used to simulate fall through results for each of the meshes and fish used in the experimental fall through data collection (Section 2.2.2.) Using the FISHSELECT software, the results obtained from all of the different penetration models were compared with the experimental fall-through results obtained. This evaluation produced a value for the degree of agreement (DA-value), which expresses the percentage fraction of the fall-through results where the simulated results came up with the same result ("yes" or "no").

2.2.4. Modelling of mesh shapes for square meshes in fish farm cages during smolt escape attempts

Before being able to use the generated virtual population of smolt and the identified smolt penetration model to predict the risk of smolt escape through square meshes in fish farm cages using the FISHSELECT methodology, an appropriate model for the semi-slack mesh state (Fig. 1b) and for the fully slack mesh state (Fig. 1c) was required. In the FISHSELECT simulation the latter is directly modelled by the condition that the smolt can escape if the circumference of its cross section under
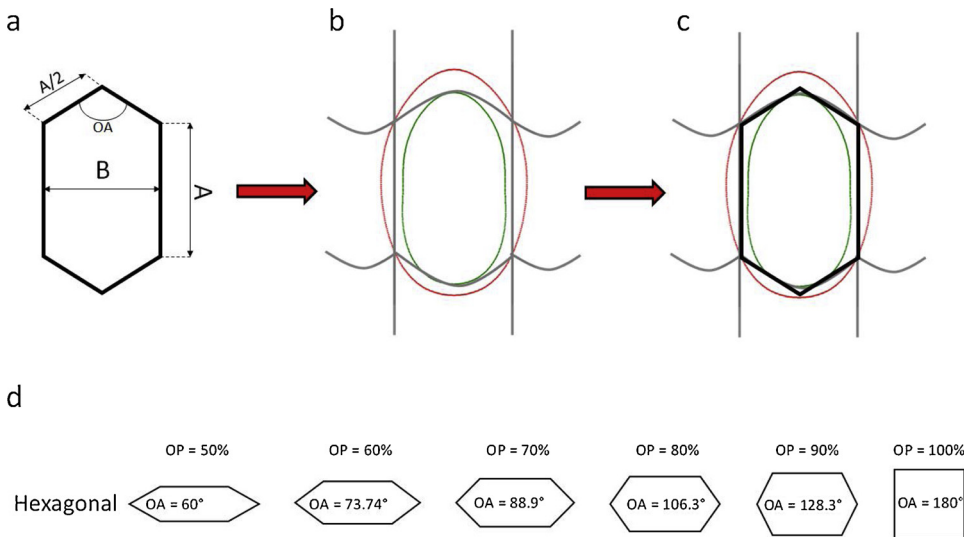
Fig. 4. Hexagonal mesh shape approximation for smolt escape through a semi-slack square mesh. "a": Details of hexagonal mesh. "b": Escape of smolt through semi-slack square mesh. "c": Approximation of the distorted semi-slack square mesh with a hexagonal shape. d: Examples of hexagonal shapes approximating distorted semi-slack square meshes with different levels of openness (see Eq. (1)).

maximum compression is less than the inner circumference of the mesh (twice the mesh size) it attempts to pass through. This is because, in this mesh state, the mesh will be fully distorted while the smolt is passing through it. In semi-slack and partly open square meshes (Fig. 1b), the shape the mesh will become when a smolt attempts to pass through was approximated by a hexagonal shape where the tensionless horizontal mesh bars are bent upwards and downwards (Fig. 4a-c). This approximation has previously successfully been applied when modelling fish escape through square mesh codends in trawl and demersal seine fisheries for several species including cod (Herrmann et al., 2016a, 2016b), haddock (Krag et al., 2011; Herrmann et al., 2016b), red mullet (Tokaç et al., 2016) and hake (Tokaç et al., 2018).

Two related measures are applied to describe the openness of a hexagonal modelled distorted semi-slack square mesh. These are the opening angle (OA) and the relative openness (OP), which quantifies the circumferential (horizontal) opening of the mesh (B) relative to the vertical opening (A) (Fig. 4a). Fig. 4d shows the relationship between OA and OP for hexagonal distorted square meshes. The relationship between OP and OA is:

$$OP = 100 \times \frac{B}{A} = 100 \times sin\left(\frac{OA}{2}\right) \tag{1}$$

The stiff mesh scenario (Fig. 1a) is a special case for the hexagonal approximation of the semi-slack mesh when OA = 180° corresponding to an OP of 100 %.

2.2.5. Quantifying the escape risk

For all three mesh scenarios (Fig. 1) the risk of smolt escape was simulated for square meshes with a mesh size between 20 and 80 mm in increments of 5 mm. For the semi-slack scenario, approximated by a hexagon, OP values from 50 to 100 % were used in increments of 5 %. Using the identified smolt penetration model, a simulation was created to determine whether each individual smolt in the virtual population could pass through the mesh in each of the mesh scenarios (stiff, semi-slack, slack). Likewise, for the standard application of the FISHSELECT method (Herrmann et al., 2009) a virtual size selection dataset for each mesh was obtained, consisting of smolt size-dependent counts of individuals (in 1 cm wide length classes) from the virtual population respectively being retained (not able to pass through) and released (being able to pass through). Then the traditional logit size selection model (2) was fitted to the size selection data by maximum likelihood estimation to obtain the values for the model parameters L50 and SR (Wileman et al., 1996).

$$logit\,(l, L50, SR) = \frac{\exp\left(\frac{ln(9)}{SR} \times (l - L50)\right)}{1 + \exp\left(\frac{ln(9)}{SR} \times (l - L50)\right)} \tag{2}$$

where *L50* quantifies the length of the smolt that have a 50 % probability of being retained. *SR* measures the steepness of the curve by the difference in *L75* and *L25* (Wileman et al., 1996). *logit* (*l, L50, SR*) provides a s-shaped curve with a monotonous increase in retention probability with increases in smolt length (Fig. 5).

Based on the obtained size selection curves, the size of a smolt having a 99 % retention probability (L99; maximum 1 % escape risk) was calculated and used as a measure for the minimum safe size of smolt that could be kept in the cages. For a logit size selection model L99 can be calculated by (Krag et al., 2014):

$$L99 = L50 + \frac{SR}{ln(9)} \times ln(99) \tag{3}$$

However, the farming industry uses smolt weight and not length. Therefore, the weight length relationship given by (4) was used. Parameters *a* and *b* were established based on least square estimation on the experimental data (length *l* (cm) versus weight *w* (g)) collected for smolt individuals acquired for the FISHSELECT analysis:

$$w = a \times l^b \tag{4}$$

Based on the above, the weight of smolt with maximum 1 % escape risk (W99) for each individual mesh was obtained by:

$$W99 = a \times L99^b \tag{5}$$

3. Results

3.1. Data collection

The data collection process was conducted at two smolt production plants in Trøndelag (Mid-Norway) from 16 to 19 June 2014. The first plant was a land-based station, while the second station was located at sea inside a fjord. All the fish in both plants belonged to the AquaGen genetic pool (Gjedrem et al., 1991). There was continuous access to live fish at both sites during the study period.

During the experimental period, the FISHSELECT procedure was applied to 127 salmon smolt, 100 of which were collected from the land-based plant. The remaining 27 were collected from the fish farm at sea and were larger in size. The size of the fish included in the study varied from 26 g (151 mm) to 240 g (295 mm) (Fig. 6).
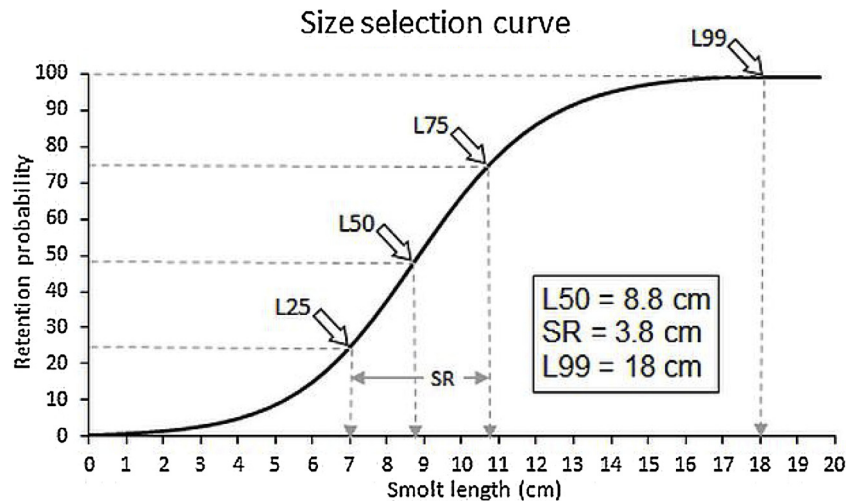
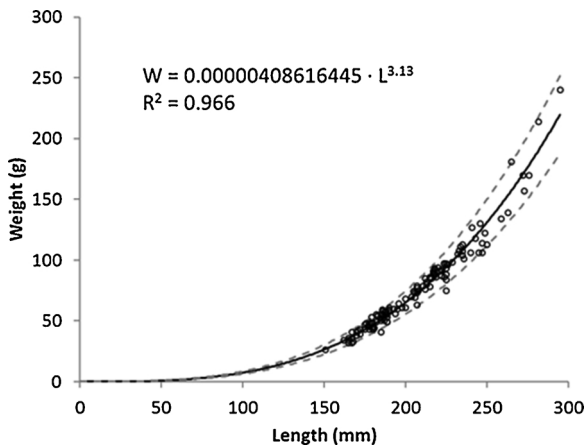**Fig. 5.** Example of a size selection curve where L50, SR and L99 are illustrated.

Fig. 6. Weight vs. length relationship for the 127 salmon smolt included in the study. $a = 4.0862 \times 10^{-6}$ and $b = 3.13$ (Eq. (4)–(5)).

3.2. Cross section model choice and compressibility of salmon smolt

After CS1 and CS2 were registered and digitized for the 127 individuals included in the study, the seven different CS models described earlier (Section 2.2.1.) were tested to determine which one would best represent CS1 and CS2. The models tested were picked based on previous experience and model choice was based on AIC (Akaike, 1974). The results in Table 1 show that the model named "flexellipse 1″ generally fitted the CS1 shapes best. The "ship" model best described the CS2 shape. Both models are 3-parameter models that exhibited a high R^2 score, which implies that the model describes the data well.

Each of the 127 smolt were tested through the 478 different meshes used in the fall-through trials. These tests produced a total of 60,706 fall-through results, which constituted the basis for determining the maximum compression levels for CS1 and CS2.

The results of the simulations showed a maximum DA of 97.52 % for the best of the CS1 models tested. For CS2, this percentage was slightly lower than for CS1 (DA = 97.35 %), for the model that scored highest. However, the highest DA value came from a model combining both CS1 and CS2 that resulted in a DA of 97.61 %. This model had a dorsal compression of 0 %, lateral compression of 15 % and ventral compression of 25 % for CS1, and a dorsal compression of 30 %, lateral compression of 20 % and ventral compression of 10 % for CS2 (Fig. 7).

3.3. Predictions of smolt escape risk from fish farms

The results from FISHSELECT were used to make predictions based on the virtual population of 5000 fish created from the acquired data. The predictions were made for square meshes of 30 and 50 mm, which are commonly used. The predictions were made for stiff non-deformable meshes, semi-slack meshes with different degrees of openness, and slack meshes Fig. 1). The results showed that for a netting with completely slack 30 mm square meshes (no tension on the netting), smolt of up to 47 g (corresponding to W99) would be able squeeze through the meshes of the netting and escape from the cage (Fig. 8a). However, if the meshes were stiff, meaning that they maintained their square shape and were not deformed in any way (constant 100 % openness), smolt weighing 23 g would be retained with no risk of escaping (< 1 %) from the cage. If the netting had semi-slack meshes, the minimum size of smolt with no risk (W99 retention probability) of escape would vary with mesh openness. The minimum weight for no risk of escape peaks at

Table 1
Comparison of the performance of the seven different models tested on the CSs (Appendix).

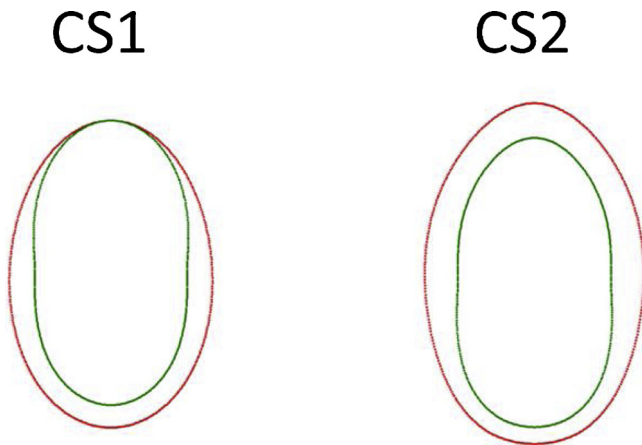| CS models | | | | | | | | | | | | | | |
|---|---|---|---|---|---|---|---|---|---|---|---|---|---|
| | Bottle | | Ellipse | | Flex Ellipse 1 | | Flex Ellipse 2 | | Flex Ellipse 3 | | Flex Drop 2 | | Ship | |
| | CS1 | CS2 | CS1 | CS2 | CS1 | CS2 | CS1 | CS2 | CS1 | CS2 | CS1 | CS2 | CS1 | CS2 |
| AIC | 152.12 | 175.01 | 162.14 | 198.62 | **146.02** | 183.79 | 157.92 | 195.26 | 156.64 | 191.1 | 148.57 | 183.01 | 148.15 | **172.36** |
| Nr parameters | 3 | 3 | 2 | 2 | 3 | 3 | 3 | 3 | 3 | 3 | 3 | 3 | 3 | 3 |
| R^2 | 0.922 | 0.976 | 0.961 | 0.969 | 0.967 | 0.974 | 0.964 | 0.971 | 0.961 | 0.971 | 0.966 | 0.974 | 0.967 | 0.976 |

Fig. 7. The combined compression model that provided the highest DA illustrated in one of the 127 smolt included in this study (the smolt was randomly selected). The red contour represents the uncompressed CS of the smolt, while the green line represents the CS of the smolt with maximum compression. (For interpretation of the references to colour in this figure legend, the reader is referred to the web version of this article).
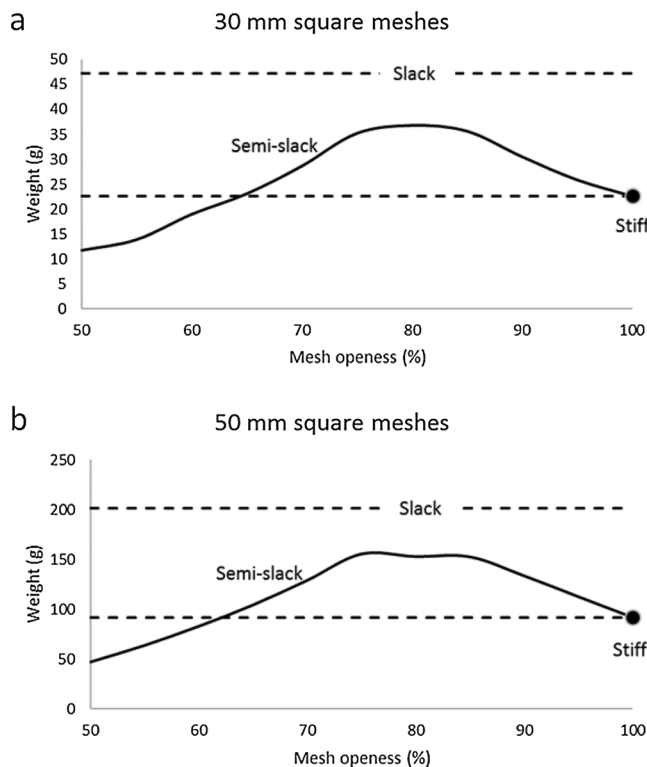

Fig. 8. Escape risk for salmon smolt of different sizes and different degrees of mesh openness. The dashed lines represent the results for slack meshes, the dot represents stiff meshes, while the solid line represents the results for semi-slack meshes. Plot "a" shows the results for 30 mm square meshes and plot "b" shows the results for 50 mm square meshes.

ca. 80 % mesh openness, as this is the point at which meshes acquire the shape that best fits the shape of the smolt CS-s and the risk of escape through the netting with semi-slack meshes would be highest (Fig. 8a).

The patterns observed for the 50 mm meshes are similar to those observed for the 30 mm meshes; however, for 50 mm meshes, the minimum size of smolt required to avoid escape through the cage meshes would be 201 g for slack meshes, 92 g for stiff meshes, and between 47 and 156 g for semi-slack meshes depending on the mesh openness (Fig. 8b). As for the 30 mm meshes, the risk of escape with the 50 mm
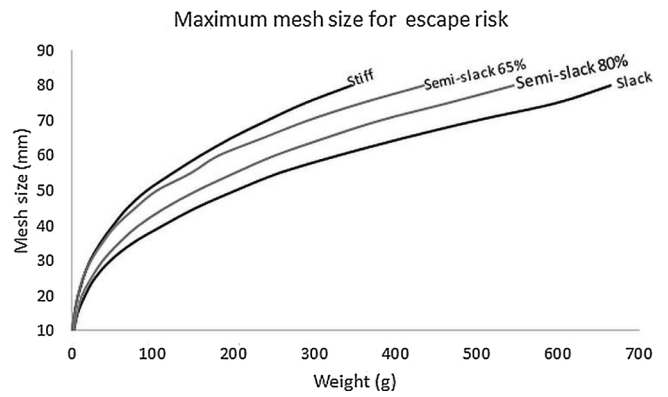

Fig. 9. Maximum square mesh size limits that guarantee less than 1 % escape risk of salmon smolt of different sizes. The lines in the plot show the limits for stiff meshes and slack meshes in black, and semi-slack meshes with 65 and 80 % mesh openness in grey.

meshes is highest when mesh openness is between 75 and 85 %.

Fig. 9 shows how the maximum safe mesh size increases with smolt size depending on mesh state. This trend is similar for stiff, semi-slack and slack meshes. The results also show that for a specific mesh size, stiff square meshes allow the use of the largest smolt sizes with no escape risk when compared to semi-slack and slack meshes (Fig. 9). The cases for semi-slack meshes represented in the plot were those with a 65 and 80 % mesh openness. As shown in Fig. 8, for the 30 and 50 mm mesh sizes, the results in Fig. 9 clearly show that at larger mesh sizes and at certain levels of mesh openness, the risk of smolt escape increases with semi-slack meshes with respect to the stiff square meshes. This risk is closest to the maximum risk, which is achieved with completely slack meshes, when the semi-slack meshes had an openness of ca. 80 %. This result is similar for square meshes of 30 and 50 mm. The results in Fig. 8 also show that the CS shape of salmon smolt is more suited to penetrate semi-slack mesh larger than 65 % mesh openness than stiff square meshes.

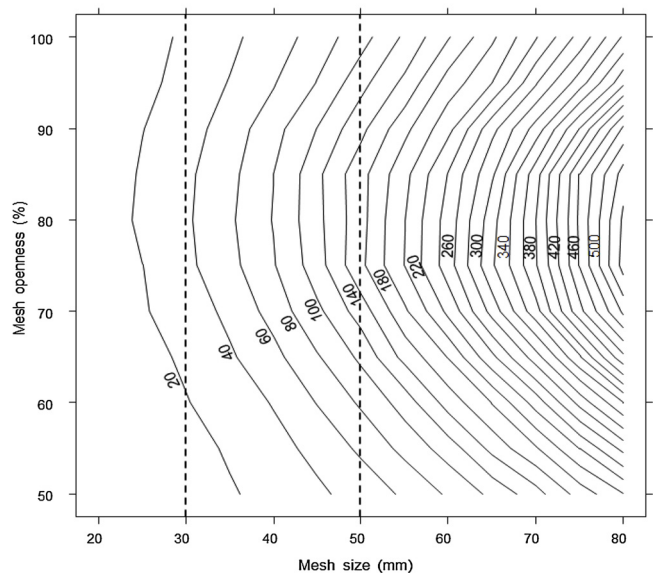The isolines in Fig. 10 show how the size of smolt with < 1 % escape

Fig. 10. Isolines showing minimum weight of salmon smolt in grams that can be used in farms for less than 1 % risk of escape for square meshes between 20 and 80 mm with mesh openness that varies between 50 and 100 % in the semi-slack mesh state. The dashed lines show the estimates for the 30 and 50 mm meshes.

risk varies through different square mesh sizes and mesh openness. A mesh with 100 % openness represents a stiff mesh, while meshes with different degrees of mesh openness represent semi-slack meshes. It is clear from the plot that at larger mesh sizes, the size of smolt has to be increased to lower the escape risk through the meshes. For example, with a mesh openness of 60 %, the increase in smolt size required when increasing mesh size from 30 to 40 mm is 40 g (from 40 to 80 g), whereas if the mesh is increased from 60 to 70 mm, the increase in smolt size required is 120 g (from 260 to 380 g).

4. Discussion

To evaluate the lower size limits of smolt that can be kept in fish farm cages, farmers and management authorities have carried out numerous trials over the last 10–15 years (Harboe and Skulstad, 2013). However, none of these trials have provided an understanding of the mechanisms involved in the potential escape of salmon smolt through fish farm cage netting. These previous trials were carried out on swimming fish or fish that were attempting to pass through a stretched panel of net meshes. The methods used did not consider the potential state of cage netting, or how the meshes may deform, when estimating the potential for salmon smolt escape. In addition, the compressibility and/or deformability of salmon smolt tissue was not assessed. In the present study, salmon smolt morphology was investigated and the minimum sizes of smolt required for different square mesh size nettings to avoid escape from farming cages was determined. The current study also illustrates for the first time how the minimum size can differ, not only with mesh size but also with mesh state and mesh openness in the cage netting.

Several studies have investigated the effect of waves (e.g. Lader et al., 2003; Tsukrov et al., 2003) and currents (e.g. Lader et al., 2008) on salmon cage netting, and have concluded that they can affect the geometry and tension of the netting, and therefore the shape of the net meshes. Considering that the fish farming industry is placing farming sites at more and more exposed locations (Bjelland et al., 2015), the effect of currents and waves on sea cage nets, and consequently on the fish retention properties is extremely important. Furthermore, many of the operations carried out by the industry require the manipulation of cage nettings, which may create situations where the netting is distorted, and fish are pressed/forced to pass through meshes in semi-slack or slack states.

The results obtained for the 30 and 50 mm nets showed that the smolt size needed to maintain a risk of escape below 1 % was approximately twice as big for slack square meshes than for stiff square meshes. This demonstrates that carrying out penetration tests on a stretched netting panel with stiff meshes can lead to a serious underestimation of the minimum size of smolt needed to avoid escape through specific meshes. The results of the current study found that for semi-slack meshes, which simulate meshes that are stiff only in one of the directions of the bars, meshes with 80 % mesh openness had the highest risk of smolt penetration, as this mesh shape best fits the CS shapes of smolt. Semi-slack meshes with 65–100 % mesh openness also exhibited a higher escape risk than stiff meshes, which again illustrates the risk of underestimating the minimum sizes of smolt needed for specific meshes, if only stiff meshes are considered.

In comparison with the results for the minimum size of fish needed with different square meshes presented in Harboe and Skulstad (2013), the results of the current study had substantially higher smolt size limits, especially for the smallest mesh sizes. Harboe and Skulstad (2013) estimated that the minimum smolt size needed for a 30 mm mesh was between 20 and 30 g, which corresponds with the risk identified in the current study when using stiff meshes. However, these sizes become seriously underestimated when mesh states other than stiff meshes are considered. Following the recommendations presented in Harboe and Skulstad (2013), the results of the current study imply a risk of smolt escape from salmon farming cages. Unlike the recommendations presented for 30 mm meshes, the recommendations presented by Harboe and Skulstad (2013) for 50 mm meshes are more in line with the escape risk for slack meshes, as presented in the current study.

The escape of farmed salmon into the wild represents a serious problem for the Norwegian fish farming industry, both economically and environmentally (Asche et al., 1999; Asche, 2008). From an environmental point of view, the problem is more serious when salmon smolt escape as opposed to adult salmon, because smolt can easily adapt to conditions in the wild and pose a threat to wild salmon stocks (Skilbrei, 2010). One of the most critical operations in fish farming with the potential for smolt escape is the setting of fish, where smolt reared in land-based plants are transferred into sea cages. At this point, it is critical to have control of the size distribution of the smolt set, as the meshes used in the netting of the sea cages should be able to retain all the smolt introduced to the cage. Despite the numerous population samples taken, the volumes of fish transferred can be so large (often several hundred thousand fish), that it is difficult to control the size distribution of the fish set and ensure that individuals below a specific size limit are not present. While the results of the current study do not directly solve the challenge of increased precision with regard to determining the size distribution of transferred smolt, they do provide clear and comprehensive smolt size limits for farmers. Furthermore, the results highlight the importance of mesh shape and mesh state. The smolt size limits presented in this study considered the morphological variability and compressibility of salmon smolt. However, in terms of the direct industrial applicability of the smolt size limits presented in this study, the fact that all fish used in the trials belonged to the AquaGen genetic pool needs to be considered. Fish from other genetic pools, or with other characteristics, could exhibit slight morphological and compressibility differences that are not considered in this study. Therefore, if minimum size limits such as those presented in this study are to be applied to salmon from different genetic pools, additional FISHSELECT analysis for a representative population of fish from that genetic pool is recommended.

Declaration of Competing Interest

The authors declare that they have no known competing financial interests or personal relationships that could have appeared to influence the work reported in this paper.

Acknowledgements

Appendix A

To describe the cross-sectional shapes of salmon smolt, FISHSELECT requires a representation in polar coordinates (θ, r), where θ is the angle (0–360 degrees) and r is the corresponding radius (see Appendix in Herrmann et al., 2009). A description that involves only a few parameters is preferred. One flexible method, which enables the modelling of a large family of different shapes using few parameters, is to use a parametric description in Cartesian coordinates of the following form (Bers and Karal, 1976):

$$x = f(t)$$
$$y = g(t)$$
, $t \in [0; 360]$

The actual shape is then defined by the selected formulas for the two functions $f(t)$ and $g(t)$.

The polar representation of the points on the surface of the cross-section is then calculated by:

$$r^2 = x^2 + y^2$$
$$\theta = tan^{-1}(y, x)$$
, where the representation returns the angle in the correct quadrant.

To represent the cross-sections of smolt, mathematical descriptions for the two functions ($f(t)$ and $g(t)$) which had as few free parameters as possible but were still able to describe the main characteristics of the cross-sectional shapes of the species were required. During initial attempts to derive a formula based on trigonometric functions in the FISHSELECT software tool, it was discovered that, apart from the ellipse, which is a standard and well-known shape with two parameters (c_1, c_2), several other descriptions with three parameters (c_1, c_2, c_3) were able to produce shapes similar to the different cross-sections of smolt. For these shapes, the functions $f(t)$ and $g(t)$ are given by:

Model	$f(t)$	$g(t)$
Bottle	$c_1 \times sin\left(\pi \times \frac{t}{180}\right) + c_1 \times c_3 \times sin\left(\pi \times \frac{t}{90}\right)$	$-c_2 \times cos\left(\pi \times \frac{t}{180}\right) + c_1 \times c_3 \times cos\left(\pi \times \frac{t}{45}\right)$
Ellipse	$c_1 \times cos\left(\pi \times \frac{t}{180}\right)$	$c_2 \times sin\left(\pi \times \frac{t}{180}\right)$
Flex Ellipse 1	$c_1 \times sin\left(\pi \times \frac{t}{180}\right)$	$-c_2 \times cos\left(\pi \times \frac{t}{180}\right) + c_3 \times cos\left(\pi \times \frac{t}{90}\right)$
Flex Ellipse 2	$c_1 \times sin\left(\pi \times \frac{t}{180}\right)$	$-c_2 \times cos\left(\pi \times \frac{t}{180}\right) + c_3 \times cos\left(\pi \times \frac{t}{60}\right)$
Flex Ellipse 3	$c_1 \times sin\left(\pi \times \frac{t}{180}\right) - c_1 \times c_3 \times sin\left(\pi \times \frac{t}{90}\right)$	$-c_2 \times cos\left(\pi \times \frac{t}{180}\right) + c_2 \times c_3 \times cos\left(\pi \times \frac{t}{90}\right)$
Flex Drop 2	$c_1 \times sin\left(\pi \times \frac{t}{180}\right) + c_1 \times c_3 \times sin\left(\pi \times \frac{t}{90}\right)$	$-c_2 \times cos\left(\pi \times \frac{t}{180}\right)$
Ship	$c_1 \times sin\left(\pi \times \frac{t}{180}\right)$	$-c_2 \times cos\left(\pi \times \frac{t}{180}\right) + c_3 \times cos\left(\pi \times \frac{t}{45}\right)$

Quantification of the ability of a particular shape to describe the experimental data for a cross section of a fish can be assessed using the R^2-value for the fit of the model to the data. The R^2-value expresses the variation in the data accounted for by the model as a fraction of the total variation in the data. By using the polar expression (θ, r) for the points along the cross section shape, the R^2-value for the shape fit can be calculated for each angle θ to compare the radius values r based on the model against those based on the experimental data. The total variation in the data is calculated as the variance in r-values from the experimental data. Thus, while the R^2-value can never exceed 1.0, a value close to 1.0 implies that the model describes the shape data well. Everything else being equal, the model resulting in the highest R^2-value is preferable. However, a more flexible model requiring a larger number of parameters to define the shape would in general be expected to produce a higher R^2-value. To be able to assess whether the improvement gained in the modelling of the shape is worth the cost of the higher number of model parameters, the mean AIC-value can be used to choose between competing models. The model with the lowest AIC-value should be preferred (Akaike, 1974). Therefore, mean R^2-values were applied for the different shape models to evaluate their ability to describe the cross-sectional shapes, while using the AIC-values to rank models with different numbers of parameters.

References

Akaike, H., 1974. A new look at the statistical model identification. IEEE Trans. Autom. Control 19, 716–722. https://doi.org/10.1109/TAC.1974.1100705. https://10.1109/TAC.1974.1100705.

Asche, F., 2008. Farming the sea. Mar. Res. Econ. 23, 527–547.

Asche, F., Guttormsen, A.G., Tveterås, R., 1999. Environmental problems, productivity and innovations in Norwegian salmon aquaculture. Aqua. Econ. Manage. 3, 19–29.

Bers, L., Karal, F., 1976. Calculus, second ed. Holt, Rinehart and Winston, New York.

Bjelland, H.V., Føre, M., Lader, P., Kristiansen, D., Holmen, I.M., Fredheim, A., Grøtli, E.I., Fathi, D.E., Oppedal, F., Utne, I.B., Schjølberg, I., 2015. Exposed Aquaculture in Norway: Technologies for Robust Operations in Rough Conditions. OCEANS'15MTS/IEEE Washington, pp. 1–10 2015.

Bridger, C.J., Fredriksson, D.W., Jensen, Ø., 2015. Physical containment approaches to mitigate potential escape of European-origin Atlantic salmon in south coast Newfoundland aquaculture operations. DFO Can. Sci. Advis. Sec. Res. Doc 2015/072.

Gjedrem, T., Gjoen, H.M., Gjerde, B., 1991. Genetic origin of Norwegian farmed Atlantic salmon. Aquaculture 98, 41–50.

Harboe, T., Skulstad, O.F., 2013. Undersøkelse Av Maskeåpning Og Smoltstørrelse. Institute of Marine Research, Nr. 22–2013. 22pp. In Norwegian). Institute of Marine Research, Postbox 1870 Nordnes, 5817 Bergen, Norway.

Herrmann, B., Krag, L., Frandsen, R., Madsen, N., Lundgren, B., Stæhr, K.J., 2009. Prediction of selectivity from morphological conditions: methodology and case study on cod (Gadus morhua). Fish. Res. 97, 59–71.

Herrmann, B., Sistiaga, M., Nielsen, K.N., Larsen, R.B., 2012. Understanding the size selectivity of redfish (Sebastes spp.) in North Atlantic trawl codends J. Northw. Atl. Fish. Sci. 44, 1–13.

Herrmann, B., Larsen, R.B., Sistiaga, M., Madsen, N.H.A., Aarsæther, K.G., Grimaldo, E., Ingolfsson, O.A., 2016a. Predicting size selection of cod (Gadus morhua) in square mesh codends for demersal seining: a simulation-based approach. Fish. Res. 184, 36–46.

Herrmann, B., Krag, L.A., Feekings, J., Noack, T., 2016b. Understanding and predicting size selection in diamond mesh codends for Danish seining: a study based on sea trials

and computer simulations. Mar. Coast. Fish. 8, 277–291.

Huang, C.-C., Tang, H.-J., Liu, J.-Y., 2006. Dynamical analysis of cage structures for marine aquaculture: numerical simulation and model testing. J. Aquac. Eng. Fish. Res. 35, 258–270.

Jensen, Ø., Dempster, T., Thorstad, E.B., Uglem, I., Fredheim, A., 2010. Escapes of fish from Norwegian sea-cage aquaculture: causes, consequences and methods to prevent escape. Aquacult. Environ. Interact. 1, 71–83.

Karlsson, S., Diserud, O.H., Fiske, P., Hindar, K., 2016. Widespread genetic introgression of escaped farmed Atlantic salmon in wild salmon populations. ICES J. Mar. Sci. 73, 2488–2498.

Keyser, F., Wringe, B.F., Jeffery, N.W., Dempson, J.B., Duffy, S., Bradbury, I.R., 2018. Predicting the impacts of escaped farmed Atlantic salmon on wild salmon populations. Can. J. Fish. Aquat. Sci. 75, 506–512.

Krag, L., Herrmann, B., Madsen, N., Frandsen, R., 2011. Size selection of haddock (Melanogrammus aeglefinus) in square mesh codends: a study based on assessment of decisive morphology for mesh penetration. Fish. Res. 110, 225–235.

Krag, L.A., Herrmann, B., Iversen, S., Engås, A., Nordrum, S., Krafft, B.A., 2014. Size selection of Antarctic krill (Euphausia superba) in trawls. PLoS One 9 (8), e102168.

Lader, P., Enerhaug, B., Fredheim, A., Krokstad, J.R., 2003. Modelling of 3D net structures exposed to waves and current. In: Eatock Taylor, R. (Ed.), Third International Conference on Hydroelasticity in Marine Technology. Department of Engineering Science. The University of Oxford, Oxford, UK.

Lader, P., Dempster, T., Fredheim, A., Jensen, Ø., 2008. Current induced net deformations in full-scale sea-cages for Atlantic salmon (Salmo salar). J. Aquac. Eng. Fish. Res. 38, 52–65.

Moe, H., Olsen, A., Hopperstad, O.S., Jensen, Ø., Fredheim, A., 2007. Tensile properties for netting materials used in aquaculture net cages. J. Aquac. Eng. Fish. Res. 37, 252–265.

Moe, H., Fredheim, A., Hopperstad, O.S., 2010. Structural analysis of aquaculture net cages in current. J. Fluid. Struct. 26, 503–516.

Moring, J.R., 1989. Documentation of unaccounted-for losses of Chinook salmon from saltwater cages. Pro. Fish. Cult. 51, 173–176.

Norwegian Directorate of Fisheries, 2018. Norwegian Directorate of Fisheries, Postbox. 185 Sentrum. 5804 Bergen, Norway. https://www.fiskeridir.no/Akvakultur/

Statistikk-akvakultur/Akvakulturstatistikk-tidsserier/Laks-regnbueoerret-og-oerret.

Norwegian Seafood council, 2018. Norwegian Seafood Council, Stortorget, Postbox 6176. 9291 Tromsø, Norway. https://seafood.no/markedsinnsikt/nokkeltall/.

Reeves, S.A., Armstrong, D.W., Fryer, R.J., Coull, K.A., 1992. The effects of mesh size, cod-end extension length and cod-end diameter on the selectivity of Scottish trawls and seines. ICES J. Mar. Sci. 49, 279–288.

Rybråten, S., Bjørkan, M., Hovelsrud, G.K., Kaltenborn, B.P., 2018. Sustainable coasts? Perceptions of change and livelihood vulnerability in Nordland, Norway. Loc. Environ. 23, 1156–1171.

Sistiaga, M., Herrmann, B., Grimaldo, E., Larsen, R.B., 2010. Assessment of dual selection in grid based selectivity systems. Fish. Res. 105, 187–199.

Sistiaga, M., Herrmann, B., Nielsen, K.N., Larsen, R.B., 2011. Understanding limits to cod and haddock separation using size selectivity in a multispecies trawl fishery: an application of FISHSELECT. Can. J. Fish. Aquat. Sci. 68, 927–940.

Skilbrei, O.T., 2010. Adult recaptures of farmed Atlantic salmon post-smolts allowed to escape during summer. Aquacult. Environ. Interact. 1, 147–153.

Tokaç, A., Herrmann, B., Gökçe, G., Krag, L.A., Ünlüler, A., Nezhad, D.S., Lök, A., Kaykaç, H., Aydın, C., Ulaş, A., 2016. Understanding the size selectivity of smolt (*Mullus barbatus*) in Mediterranean trawl codends: a study based on fish morphology. Fish. Res. 174, 81–93.

Tokaç, A., Herrmann, B., Gökçe, G., Krag, L.A., Nezhad, D.S., 2018. The influence of mesh size and shape on the size selection of European hake (*Merluccius merluccius*) in demersal trawl codends: an investigation based on fish morphology and simulation of mesh geometry. Sci. Mar. 82, 147–157.

Tsukrov, I., Eroshkin, O., Fredriksson, D., Swift, M.R., Celikkol, B., 2003. Finite element modelling of net panels using a consistent net element. Ocean Eng. 30, 251–270.

Wienbeck, H., Herrmann, B., Moderhak, W., Stepputtis, D., 2011. Effect of netting direction and number of meshes around on size selection in the codend for Baltic cod (*Gadus morhua*). Fish. Res. 109, 80–88.

Wileman, D., Ferro, R.S.T., Fonteyne, R., Millar, R.B. (Eds.), 1996. Manual of Methods of Measuring the Selectivity of Towed Fishing Gears. ICES Cooperative Research report No. 215.